MEDDOCS Open Access Publisher

ISSN: 2578-8760

Journal of Nanomedicine

Open Access | Research Article

Lipid Composition Design of Lipid Nanoparticles by Bayesian Optimization for High-Efficiency Gene Delivery to Peripheral Blood Mononuclear Cells

Emi Nozaki[1]; Eiichi Akahoshi[1]; Arisa Fukui[1]; Hidekazu Saito[2]; Daiki Kiribuchi[2]; Takeichiro Nishikawa[2]; Katsuyuki Naito[3]; Mitsuko Ishihara-Sugano[1]*

[1]Frontier Research Laboratory, Nano Materials and Frontier Research Laboratories, Corporate Research and Development Center, Toshiba Corporation, Japan.

[2]System AI Laboratory, Advanced Intelligent Systems Laboratories, Corporate Research and Development Center, Toshiba Corporation, Japan.

[3]Transducer Technology Laboratory, Nano Materials and Frontier Research Laboratories, Corporate Research and Development Center, Toshiba Corporation, Japan.

***Corresponding Author(s): Mitsuko Ishihara-Sugano**
Frontier Research Laboratory, Nano Materials and Frontier Research Laboratories, Corporate Research and Development Center, Toshiba Corporation, Japan.
Tel: +81- 44-549-2182, Fax: +81-44-549-2202;
Email: mitsuko.sugano@toshiba.co.jp

Received: Dec 03, 2020

Accepted: Jan 20, 2021

Published Online: Jan 22, 2021

Journal: Journal of Nanomedicine

Publisher: MedDocs Publishers LLC

Online edition: http://meddocsonline.org/

Keywords: Gene delivery; Lipid nanoparticles; Lipid composition; Human peripheral blood mononuclear cells; Bayesian optimization.

Abstract

Lipid Nanoparticles (LNPs), which consist mainly of cationic lipids, are considered a promising gene delivery tool for gene therapy with advantages such as ease of manufacturing and reduced toxicity. Human Peripheral Blood Mononuclear Cells (hPBMCs) are an important raw material for gene therapy and there is a need to develop tools for effectively delivering genes to them. LNPs are expected to be a suitable delivery tool for this purpose. LNPs are unique in that their membrane structure can be flexibly changed according to the target cell by changing their lipid ratio. To maximize the efficiency of gene delivery to hPBMCs, we applied a Bayesian Optimization (BO) method to design an LNP composed of the newly synthesized cationic lipids FFT-10 and FFT-20. BO can predict the optimum value from a small number of trials and is also useful for multifactor optimization. Consequently, we found a lipid composition that was 260-fold more efficient than the initial composition by using BO combined with experimental trials. In conclusion, BO can provide beneficial results for constructing the lipid composition of LNPs for target cells in order to expand the clinical application. It is thus important to design LNPs that offer highly efficient gene delivery to hPBMCs.

Cite this article: Nozaki E, Akahoshi E, Fukui A, Saito H, Kiribuchi D, et al. Lipid composition design of lipid nanoparticles by Bayesian optimization for high-efficiency gene delivery to peripheral blood mononuclear cells. J Nanomed. 2021; 4(1): 1033.

Introduction

Gene therapy is a promising treatment for diverse genetic diseases such as cancer, hemophilia, and neurodegenerative diseases [1-4]. Gene therapy is based on the delivery of exogenous genes into pathological cells to modify the expression of some particular genes to treat or prevent a disease. Therefore, the successful clinical application of gene therapy depends on establishing a highly efficient gene delivery system to pathological cells.

Over the past few decades, many gene delivery systems have been developed, and virus-based delivery systems have been widely used in clinical applications. It was reported that virus-based delivery systems were used in about 70% of gene therapy clinical trials in 2017 [5]. Although virus-based delivery systems have high gene delivery efficiency, they are known to be highly immunogenic and thus present safety concerns [6]. Therefore, the development of an effective and safe non-viral gene delivery system for gene therapy remains a problem to be addressed.

Since the first clinical application of a non-viral gene delivery system using cationic lipids [7], progress has continued with the application of lipid nanoparticles (LNPs), which offer advantages such as safety, low-cytotoxicity, and stability. LNPs are usually made from cationic lipids, structural lipids, cholesterol, and PEG lipids [8]. In particular, many cationic lipids are newly designed by changing the polarity of the polar head and the carbon number and degree of unsaturation of the fatty acid tail, and this has been reported to affect the gene delivery efficiency [9-11]. In addition, recent studies have shown that the lipid composition of LNPs change the structure and pKa of LNPs, which affects the gene delivery efficiency to diverse cells [9].

To design the lipid composition of LNPs to maximize the gene delivery efficiency to target cells, it is necessary to optimize the kinds and molecular ratios of the lipids. In this work, we report that a combination approach consisting of biological experiments and machine learning is effective for customizing the lipid composition of LNPs.

Bayesian Optimization (BO), which is a machine learning technique, makes it possible to determine the optimum composition despite limited materials information and limited numbers of trials [12,13]. BO recommends not only points of high expectation but also points of high uncertainty as search candidates by using an objective function (acquisition function) that considers both exploration and exploitation based on the surrogate model obtained by learning the experimental results [12,14]. Recently, the effects of BO have been demonstrated in production process optimization and material design in which many factors are complexly correlated [15-18]. For example, it was reported that BO was effective in a hybrid organic–inorganic perovskite design that optimizes the perovskite structure of solar cells [19]. Similar to the multicomponent optimization of inorganic material, we examined the lipid composition of LNPs that maximized the efficiency of gene delivery to target cells by using BO.

Human Peripheral Blood Mononuclear Cells (hPBMCs) are a mixture of various immune cells separated from peripheral blood and are used for preclinical assays, including natural killer cytotoxicity assays, leukocyte recruitment, adhesive interactions with endothelial cells, suppression assays, and lymphocyte proliferation assays [20]. hPBMCs are also very important as starting material for gene therapy, including T-Cell Receptor T-Cell Therapy (TCR-T) and Chimeric Antigen Receptor T-Cell Therapy (CAR-T) [21]. Viral vectors are commonly used for T-cell gene therapy because of their high gene delivery efficiency [22], but there is a risk of high immunogenicity. Therefore, the application of non-viral gene delivery systems such as LNPs to T-cell gene therapy may contribute to improving the safety of T-cell gene therapy. Billingsley et al. reported on using LNPs to deliver genes into hPBMCs, but the gene expression level was not sufficient for gene therapy [23]. LNPs need to be designed to allow the gene to reach hPBMCs and be sufficiently expressed.

In this study, we used a method involving BO in order to design a more effective lipid composition for LNPs to deliver genes to hPBMCs.

Materials and methods

Lipids

The functional lipids FFT-10 and FFT-20 were synthesized as described in the supplementary material (Figure S-1 and Figure S-3). DOPE (1, 2-dioleoyl-sn-glycero-3-phosphoethanolamine) and DOTAP (1, 2-dioleoyl-3-trimethylammonium-propane chloride salt) were purchased from Avanti Polar Lipids, Inc (USA). Cholesterol was purchased from Sigma-Aldrich (USA). DMG-PEG 2000 (1, 2-dimyristoyl-rac-glycero-3-methylpolyoxyethylene) was purchased from NOF Corporation (Japan).

Plasmid DNA

To construct pCMV-nLuc plasmid encoding NanoLuc, NanoLuc sequence from pNL1.1 (Promega, USA) was subcloned into pcDNA4/V5-His B (Thermo Fisher Scientific, USA) digested with Hind III and Xba I restriction endonucleases (Takara Bio, Japan).

Peptides

The mHP-1 peptide (RQRQRYYRQRQRGGRRRRRR) and the mHP-2 peptide (RRRRRRYYRQRQRGGRRRRRR) were chemically synthesized (Polypeptide, USA).

Cell culture

Human Peripheral Blood Mononuclear Cells (hPBMCs, Lonza, Switzerland) were maintained in TexMACS medium (Miltenyi Biotec, Germany) containing deoxyribonuclease I (Worthington, USA), human interleukin-7 (IL-7, Miltenyi Biotec, Germany) and human interleukin-15 (IL-15, Miltenyi Biotec, Germany), and cultured in an incubator at 37 °C with 5% CO_2. The cells were activated by CD3 antibody (Miltenyi Biotec, Germany) and CD28 antibody (Miltenyi Biotec, Germany). At 24 h after activation, the cells were prepared for transfection by LNPs.

Preparation of lipid nanoparticles (LNPs)

pDNA and peptide solutions (0.255 mg/ml and 0.15 mg/ml) were prepared in 10 mM HEPES (pH 7.3, Dojindo, Japan). DNA particles were prepared by dropping the pDNA solution into the peptide solution under vortexing. Lipids were dissolved in a solution of ethanol and mixed DNA particles under vortexing. The solution was further diluted by adding 10-fold amount of 10 mM HEPES (pH 7.3). The diluted solution was concentrated by ultrafiltration using Amicon Ultra 0.5 Ultracel-50 50 kDa (Merck, Germany).

Measurement of particle size and zeta potential

The particle size and zeta potential of the LNPs were measured using a Zetasizer Nano ZSP (Malvern, UK). The measure-

ment data were analyzed by the software supplied with the device.

Low-voltage transmission electron microscopy

To observe the structure of the LNPs, we applied the LNP solution to a grid without staining and observed it by a low-voltage transmission electron microscopy (LV-TEM) (LVEM5D; Delong Instruments, Czech Republic) at 5 kV.

Gene delivery to hPBMCs

The plasmid DNA was delivered to hPBMCs by using LNPs or Lipofectamine 3000 (Thermo Fisher Scientific, USA). The day before transfection, hPBMCs were seeded in 96-well plates at 4.0×10^5 cells/well and activated with CD3 and CD28 antibodies. LNPs or transfection reagents were added to hPBMCs so that the amount of plasmid DNA was 0.5 μg/well. Transfected hPBMCs were cultured in an incubator at 37 °C with 5% CO_2 for 48 h.

Luciferase assay

The expression intensity of plasmid DNA (pCMV-nLuc) delivered to hPBMCs by LNPs or Lipofectamine 3000 (Thermo Fisher Scientific, USA) was measured using Nano-Glo Luciferase Assay (Promega, USA) and a plate reader (infinite F200 PRO; Tecan, Switzerland) according to the manufacturer's instructions.

Measurement of cell viability

To compare the cytotoxicity of LNPs or lipofection reagent, the cell viability of transfected hPBMCs was measured by trypan blue staining. After mixing the cell suspension with an equal amount of trypan blue stain solution, the number of viable cells was measured by an automated cell counter (Countess II FL; Thermo Fisher Scientific, USA). The relative cell viability of transfected hPBMCs was calculated such that the number of viable cells of untransfected hPBMCs was 100%.

Normalization

Luciferase activity and cell viability of hPBMCs were normalized to those of the control LNP. The lipid composition of the control LNP had a molecular ratio of FFT-10, FFT-20, DOPE, DOTAP, cholesterol, and DMG-PEG was 32%, 0%, 5%, 9%, 51%, and 3%, respectively. The measurement results of each sample were normalized based on cell viability and luciferase activity of hPBMCs transfected with the control LNP.

Statistics

All values are presented as means ± standard deviation (SD). All experiments were replicated at least three times. Data were analyzed using the Tukey–Kramer test with the Excel software package.

Results & discussion

Previous structure-activity relationship studies have shown that to promote formulation of LNPs, the lipids need to have an amphipathic structure with a hydrophilic head group containing ionizable amine and long hydrophobic dialkyl chains. The ionizable amine plays an important role in escaping the endosomal compartment following endocytosis uptake of LNPs into cells [24-26]. Tertiary amines have been reported to have a relatively strong proton sponge effect within ionizable amine [27,28]. We therefore designed new functional amino lipids (FFT-10 and FFT-20) having a hydrophilic head group containing two tertiary amines. Figure 1 shows the structures of FFT-10 and FFT-20.

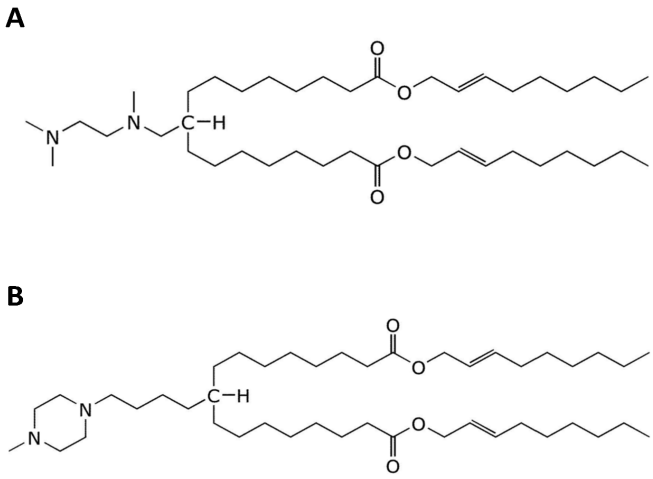

Figure 1: Chemical structure of (A) FFT-10 and (B) FFT-20.

Table 1: Molecular ratio of the lipid composition and the luciferase activity of LNP-1, LNP-2, LNP-3, and Lipofectamine 3000.

	Molecular ratio of the lipid composition (% mol)						Luciferase activity (RLU/well)
	FFT-10	FFT-20	DOPE	DOTAP	Cholesterol	DMG-PEG	
LNP-1	0	0	28	28	41	3	146 ± 63
LNP-2	33	0	19	19	27	2	3536 ± 93*
LNP-3	0	33	19	19	27	2	6147 ± 810*
Lipofectamine 3000							224 ± 44

Data are means ± SD (n=3). Statistically significant differences (*P < 0.05, Tukey-Kramer test).
*: in comparison with LNP-1 and Lipofectamine 3000

We prepared three LNPs encapsulating the plasmid DNA (pCMV-nLuc). The lipid compositions of these LNPs are shown in Table 1. Using these LNPs or Lipofectamine 3000, the plasmid DNA (pCMV-nLuc) was delivered to the hPBMCs, and we compared the luciferase activity of the cells in terms of gene delivery efficiency. As shown in Table 1, LNP-2 and LNP-3, which were composed of our new lipids (FFT-10 and FFT-20), had higher luciferase activity compared with LNP-1 and Lipofectamine 3000. We subsequently prepared LNPs containing both FFT-10 and FFT-20 and measured the luciferase activity of the cells (Table 2). Comparing the luciferase activities of LNP-4, LNP-5, and LNP-6, small variations in the molecular ratio of the lipid composition were found to affect the gene delivery efficiency.

Table 2: Molecular ratio of the lipid composition and the luciferase activity of LNP-4, LNP-5, and LNP-6.

	Molecular ratio of the lipid composition (% mol)						Luciferase activity (RLU/well)
	FFT-10	FFT-20	DOPE	DOTAP	Cholesterol	DMG-PEG	
LNP-4	25	15	19	6	32	3	146481 ± 29542
LNP-5	24	14	21	8	31	2	118950 ± 24839
LNP-6	22	15	21	8	32	2	288243 ± 55693*

Data are means ± SD (n=3). Statistically significant differences (*P < 0.05, Tukey-Kramer test).
*: in comparison with LNP-4 and LNP-5

This result shows that it is necessary to optimize the lipid composition and molecular ratio in parallel for target cells in order to maximize the gene delivery efficiency of LNPs.

BO is a machine learning technique that has been reported to be effective in production process optimization and material design, which has many are complexly correlated factors [14-17]. We therefore attempted to apply BO to the identification of the optimum lipid composition and molecular ratio of LNPs. The process was performed as follows (Figure 2):

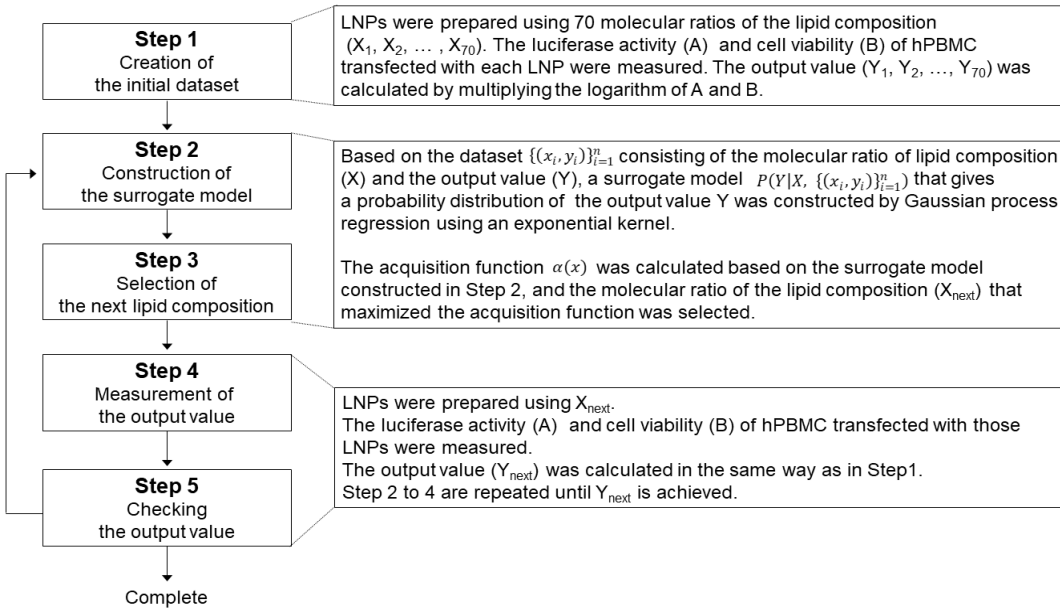

Figure 2: Process of lipid composition design using Bayesian optimization.The five steps are (1) creating the initial dataset; (2) constructing the surrogate model; (3) selecting the next lipid composition; (4) measuring the output value; and (5) checking the output value. These steps are repeated until the output value is achieved.

Step 1: Creation of the initial dataset

We set the search range for the lipid composition such that FFT-10 was from 0 to 74 nmol, FFT-20 was from 0 to 74 nmol, DOPE was 0 to 42 nmol, DOTAP was 0 to 42 nmol, cholesterol of 0 to 90 nmol, and DMG-PEG was 0 to 6 nmol. We designed 70 different molecular ratios of the lipid composition (X) based on the experimental design (Supplementary Table S1, Nos. 1-70). LNPs were prepared using these 70 molecular ratios, and the luciferase activity and cell viability of hPBMCs transfected with each LNP were measured. The output value (Y) was calculated by multiplying the logarithm of the luciferase activity with the cell viability of hPBMCs.

Step 2: Construction of the surrogate model of the output value (Y) using the dataset

Based on the dataset $\{(x_i, y_i)\}_{i=1}^n$ consisting of the molecular ratio of lipid composition (X) and the output value (Y), a surrogate model $P(Y \mid X, \{(x_i, y_i)\}_{i=1}^n)$ that gives a probability distribution of the output value Y was constructed by Gaussian process regression using an exponential kernel.

Step 3: Selection of the next molecular ratio of lipid composition (X_{next})

The acquisition function $\alpha(x)$ was calculated based on the surrogate model constructed in Step 2, and the molecular ratio of the lipid composition (X_{next}) that maximized the acquisition function was selected. We used expected improvement as the acquisition function.

Step 4: Measurement of the output value (Y_{next})

We prepared LNPs with the molecular ratio for lipid composition (X_{next}) selected in Step 3, and measured the luciferase activity and cell viability of hPBMCs transfected with those LNPs. The output value (Y_{next}) was calculated in the same way as in Step 1.

Step 5: Updating the dataset and repeating Steps 2 to 4

The surrogate model was updated using the dataset containing the additional data from Step 4, and the new molecular ratio of the lipid composition that maximized the acquisition function was selected. We examined the optimum lipid composition for hPBMCs by repeating Steps 2 to 4 (Supplementary Table S1,

Nos. 71–102).

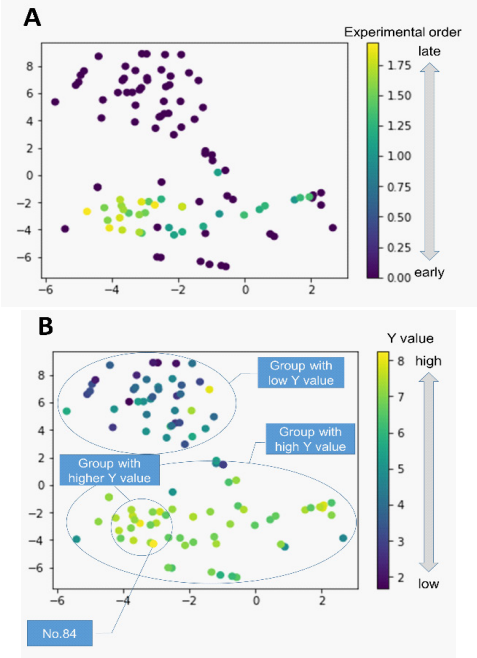

Figure 3: BO solution space visualized by projecting the six-dimensional lipid composition onto a two-dimensional space. (A) Distribution of LNPs based on the experimental order of BO. (B) Distribution of LNPs based on the output value Y.

Figure 3 shows the scheme for exploring the lipid composition using BO. The BO solution space was visualized by projecting the six-dimensional lipid composition onto a two-dimensional space. Dimension reduction was performed using the t-SNE algorithm [29]. Figure 3-A shows the BO trial order on a heat map, which progresses toward the lower left. Figure 3-B shows the output value Y of each LNP as a heat map projected onto the same two-dimensional space. From the result that a lipid composition with a higher Y value was proposed after the learning progressed, it was considered that the lipid composition selected by BO was performed correctly. The BO method selected the same composition as Nos. 70 and 84, in which the molecular ratio of FFT-10, FFT-20, DOPE, DOTAP, cholesterol, and DMG-PEG (16%, 16%, 18%, 9%, 39%, and 2%, respectively) was thought to be optimal for gene delivery to hPBMCs. To confirm the gene delivery efficiency of this composition, we prepared LNP-7 encapsulating the plasmid DNA (pCMV-nLuc) and compared the luciferase activity with LNP-7 with that with LNP-2 and LNP-3, as shown in Table 3.

Table 3: Molecular ratio of the lipid composition, and the particle size, zeta potential, and luciferase activity of LNP-2, LNP-3, and LNP-7.

	Molecular ratio of the lipid composition (% mol)						Particle size (d.nm)	Zeta potential (mV)	Luciferase activity (RLU/well)
	FFT-10	FFT-20	DOPE	DOTAP	Cholesterol	DMG-PEG			
LNP-2	33	0	19	19	27	2	152.5 ± 1.4	49.7 ± 2.9	4078 ± 201
LNP-3	0	33	19	19	27	2	165.4 ± 0.2	58.2 ± 2.8	6797 ± 750
LNP-7	16	16	18	9	39	2	201.0 ± 1.0	52.0 ± 1.6	1790531 ± 62502*

Data are means ± SD (n=3). Statistically significant differences (*P < 0.05, Tukey-Kramer test).
*: in comparison with LNP-2 and LNP-3

The luciferase activity with LNP-7 was 430 times that of LNP-2 and 260-fold that of LNP-3. Since LNP-7 can be considered to be the optimal lipid composition for delivering the gene to hPBMCs, the selection method in combination with BO is considered to be appropriate for optimization of multiple compositions.

To analyze correlations between the structures and gene delivery efficiencies of the LNPs, the LNPs were observed by LV-TEM (5 kV) without staining. LV-TEM is an effective imaging tool for biological materials. The improved contrast of LV-TEM eliminates heavy metal negative stains that can cause imaging artifacts in samples containing light elements such as LNPs. By using LV-TEM, we considered that it would be possible to observe the structure of LNPs that are close to the negative state.

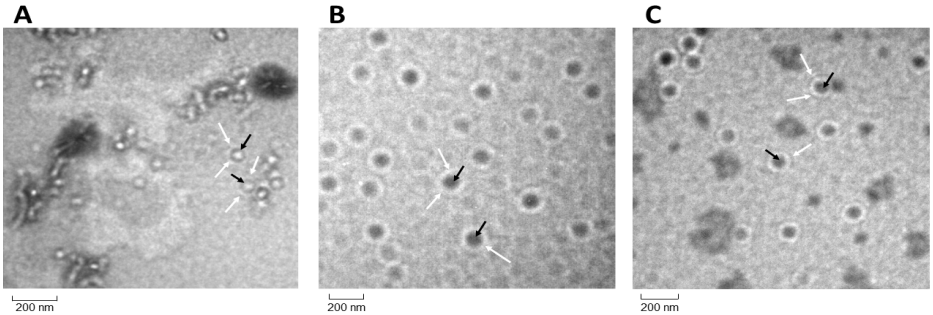

Figure 4: Structure of LNPs observed by low voltage (5 kV) transmission electron microscopy. (A) Structure of LNP-2. Black arrows indicate layers with a relatively high electron density. White arrows indicate indistinct layers of the outermost layer. (B) Structure of LNP-3. Black arrows indicate high-electron-density cores. White arrows indicate low-electron-density layers. (C) Structure of LNP-7. Black arrows indicate a high-electron-density cores. White arrows indicate low-electron-density layers.

As shown in Figure 4-A, LNP-2 consisted of a white low-electron-density core surrounded by a layer with a relatively high electron density (black arrows), and an indistinct layer (white arrows) was observed in the outermost layer. By comparison, LNP-3 (Figure 4-B) and LNP-7 (Figure 4-C) had a relatively clear structure with a core having a high electron density (black arrows) covered by a low-electron-density layer (white arrows). In addition, it was observed that the outer layer of LNP-7 had a clearer edge than that of LNP-3. It was considered that the layer with the high electron density contains mainly plasmid DNA, and the layer with the low electron density contains mainly lipids [30]. It is possible that differences in the outermost structure that is in contact with the cells affects the gene delivery efficiency of LNPs [31].

Conclusion

It is thought that in LNPs containing multiple lipids, not only the individual lipids but also the interactions between lipids, affected the gene delivery efficiency of LNPs based on their structures. The BO method that was used in this study was useful in this case where multiple components mutually influence each other because it is a so-called "black box optimization method". Although a function that associates the molecular ratio of lipid composition with the gene delivery efficiency was not elucidated, the maximum value was nevertheless predicted. The method used in this study that combines experimental methods with BO was effective for the construction of the lipid composition for LNPs for target cells.

We designed an optimal lipid composition for LNPs for gene delivery to hPBMCs. The BO framework we presented in this paper was suitable and effective for application to the design of multicomponent LNPs. Application of this method to the design of clinically usable LNPs requires improving the accuracy of machine learning and accumulating more examples of cell applications.

References

1. Amer MH. Gene therapy for cancer: present status and future perspective. Mol Cell Ther. 2014; 2: 27-45.
2. Shu SA, Wang J, Tao MH, Leung PSC. Gene therapy for autoimmune disease. Clin Rev Allergy Immunol. 2015; 49: 163-176.
3. Makris M. Hemophilia gene therapy is effective and safe. Blood. 2018; 131(9): 952-953.
4. Chen W, Hu Y, Ju D. Gene therapy for neurodegenerative disorders: Advances, insights and prospects. Acta Pharm Sin B. 2020.
5. Ginn SL, Amaya AK, Alexander IE, Edelstein M, Abedi MR. Gene therapy clinical trials worldwide to 2017: An update. J Gene Med 2018; 20: e3015.
6. Patil S, Gao YG, Lin X, Li Y, Dang K, et al. The Development of Functional Non-Viral Vectors for Gene Delivery. Int J Mol Sci. 2019; 20: 5491-5513.
7. Felgner PL. Improvements in Cationic Liposomes for In Vivo Gene Transfer. Human Gene Therapy. 1996; 7: 1791-1793.
8. Cullis PR, Hope MJ. Lipid nanoparticle systems for enabling gene therapies. Mol Ther. 2017; 25: 1467-1475.
9. Sato Y, Okabe N, Note Y, Hashiba K, Maeki M, et al. Hydrophobic scaffolds of pH-sensitive cationic lipids contribute to miscibility with phospholipids and improve the efficiency of delivering short interfering RNA by small-sized lipid nanoparticles. Acta Biomater. 2020; 102: 341-350.
10. Akita H, Ishiba R, Hatakeyama H, Tanaka H, Sato Y, et al. A neutral envelope-type nanoparticle containing pH-responsive and SS-cleavable lipid-like material as a carrier for plasmid DNA. Adv Healthc Mater. 2013; 2: 1120-1125.
11. Jayaraman M, Ansell SM, Mui BL, Tam YK, Chen J. Maximizing the potency of siRNA lipid nanoparticles for hepatic gene silencing In Vivo. Angew Chem Int Ed Engl. 2012; 51: 8529-8533.
12. Shahriari B, Swersky K, Wang Z, Adams RP, Freitas N, et al. Taking the human out of the loop: a review of Bayesian optimization. Proc IEEE. 2016; 104: 148-175.
13. Ueno T, Rhone TD, Houc Z, Mizoguchi T, Tsuda K. COMBO: An efficient Bayesian optimization library for materials science. Materials Discovery 2016; 4: 18-21.
14. Brochu E, Cora VM, Freitas N. A tutorial on Bayesian optimization of expensive cost functions, with application to active user modeling and hierarchical reinforcement learning. Department of computer science, The University of British Columbia. Technical report TR-2009-023.
15. Toyoura K, Hirano D, Seko A, Shiga M, Kuwabara A, et al. A machine learning-based selective sampling procedure for identifying the low energy region in a potential energy surface: a case study on proton conduction in oxides. Physical Review B. 2016; 93: 054112.
16. Yamawaki M, Ohnishi M, Ju S, Shiomi J. Multifunctional structural design of grapheme thermoelectrics by Bayesian optimization. Science Advances. 2018; 4: eaar4192.
17. Ju S, Shiga T, Feng L, Hou Z, Tsuda K, et al. Designing nanostructures for phonon transport via Bayesian optimization. Phys Rev X. 2017; 7: 021024.
18. Zhang Y, Apley DW, Chen W. Bayesian optimization for materials design with mixed quantitative and qualitative variables. Scientific Reports. 2020; 10: 4924.
19. Herbol HC, Hu W, Frazier P, Clancy P, Poloczek M. Efficient search of compositional space for hybrid organic–inorganic perovskites via Bayesian optimization. Npj Computational Materials. 2018; 4: 51.
20. Betsou F, Gaignaux A, Ammerlaan W, Norris PJ, Stone M. Biospecimen science of blood for peripheral blood mononuclear cell (PBMC) functional applications. Curr Pathbiol Rep. 2019; 7: 17-27.
21. Burger SR, Juliano L, Wang W. Cellular raw material collection in cell therapy: critical determinant of product quality. Drug Discovery World. 2014; 15: 29-34.
22. Park JH, Geyer MB, Brentjens RJ. CD19-targeted CAR T-cell therapeutics for hematologic malignancies: interpreting clinical outcomes to date. Blood. 2016; 127: 3312-3320.
23. Billingsley MM, Singh N, Ravikumar P, Zhang R, June CH, et al. Ionizable lipid nanoparticle-mediated mRNA delivery for human CAR T cell engineering. Nano Lett. 2020; 20: 1578-1589.
24. Hoekstra D, Rejman J, Wasungu L, Shi F, Zuhorn I. Gene delivery by cationic lipids: in and out of an endosome. Biochem Soc Trans. 2007; 35: 68-71.
25. Sarker SR, Takeoka S. Amino acid-based liposomal assemblies: Intracellular plasmid DNA delivery nanoparticles. J Nanomed. 2018; 2: 1008-1022.
26. Rejman J, Bragonzi A, Conese M. Role of clathrin- and caveolae-mediated endocytosis in gene transfer mediated by lipo- and polyplexes. Mol Ther. 2005; 12: 468-474.
27. Sonawane ND, Szoka FCJr, Verkman AS. Chloride accumulation

and swelling in endosomes enhances DNA transfer by polyamine-DNA polyplexes. J Biol Chem. 2003; 278: 44826-44831.

28. Freeman EC, Weiland LM, Meng WS. Modeling the proton sponge hypothesis: examining proton sponge effectiveness for enhancing intracellular gene delivery through multiscale modeling. J Biomater Sci Polym Ed. 2013; 24: 398-416.

29. Maaten LVD, Hinton G. Visualizing data using t-SNE. J Mach Learn Res. 2008; 9: 2579-2605.

30. Huo S, Gong N, Jiang Y, Chen F, Guo H, et al. Gold-DNA nanosunflowers for efficient gene silencing with controllable transformation. Sci Adv. 2019; 5: eaaw6264.

31. Shen Z, Nieh MP, Li Y. Decorating Nanoparticle Surface for Targeted Drug Delivery: Opportunities and Challenges. Polymers 2016; 8: 83-100.